Publications of the Astronomical Society of Australia (PASA), Vol. 33, e036, 9 pages (2016).

doi:10.1017/pasa.2016.30

A Dynamical Gravitational Wave Source in a Dense Cluster

Jarrod R. Hurley[1,3,4], Anna C. Sippel[2], Christopher A. Tout[3] and Sverre J. Aarseth[3]

[1]Centre for Astrophysics and Supercomputing, Swinburne University of Technology, P.O. Box 218, VIC 3122, Australia
[2]Max Planck Institute for Astronomy, Königstuhl 17, 69117 Heidelberg, Germany
[3]Institute of Astronomy, University of Cambridge, Madingley Road, Cambridge, CB3 0HA, UK
[4]Email: jhurley@swin.edu.au

(Received May 17, 2016; Accepted July 20, 2016)

Abstract

Making use of a new *N*-body model to describe the evolution of a moderate-size globular cluster, we investigate the characteristics of the population of black holes within such a cluster. This model reaches core-collapse and achieves a peak central density typical of the dense globular clusters of the Milky Way. Within this high-density environment, we see direct confirmation of the merging of two stellar remnant black holes in a dynamically formed binary, a gravitational wave source. We describe how the formation, evolution, and ultimate ejection/destruction of binary systems containing black holes impacts the evolution of the cluster core. Also, through comparison with previous models of lower density, we show that the period distribution of black hole binaries formed through dynamical interactions in this high-density model favours the production of gravitational wave sources. We confirm that the number of black holes remaining in a star cluster at late times and the characteristics of the binary black hole population depend on the nature of the star cluster, critically on the number density of stars and by extension the relaxation timescale.

Keywords: binaries: close – globular clusters: general – gravitational waves – methods: numerical – stars: kinematics and dynamics

1 INTRODUCTION

The recent detection of gravitational waves (GWs) (Abbott et al. 2016a) believed to be from the merging of two black holes (BHs) has invigorated the modelling community and led to a new set of papers on BH–BH merging rates expected from star cluster populations (Chatterjee, Rodriguez, & Rasio 2016; Mapelli 2016; Rodriguez et al. 2016a, 2016b) and field binaries (Belczynski et al. 2016a; Eldridge & Stanway 2016). These studies build on work over the past decade or more that focussed on predictions for the Laser Interferometric Gravitational-wave Observatory (LIGO) and Advanced LIGO detections of the merging of double compact object binaries with population synthesis of binary stars (e.g. Belczynski, Kalogera, & Bulik 2002; Dominik et al. 2015) and models of the dense star cluster environment (e.g. Portegies Zwart & McMillan 2000; Downing et al. 2011; Antonini et al. 2016).

The GW source GW150914 is the first detection of its kind and also the first observational evidence for the merging of a BH–BH binary (Abbott et al. 2016a). The component masses are derived to be 36 and 29 $M_\odot$ based on signal matching the waveform expected for the inspiral and merge of these BH masses. It has been suggested that a globular cluster (GC) environment is the most likely place to form such a high-mass BH binary (Rodriguez et al. 2016b) but pathways exist for normal binary evolution in the field as well (Belczynski et al. 2016a; see also the discussion in Dvorkin et al. 2016). More recently, a second source GW151226 has been announced (Abbott et al. 2016b) with derived masses of 14.2 and 7.5 $M_\odot$ (although with sizeable error bars). Previous studies have examined how a population of BHs may evolve in a star cluster (see Breen & Heggie 2013 and Chatterjee et al. 2016 for recent summaries). In essence, many BHs are expected to form in a typical GC and these BHs quickly form a centralised subsystem which may be unstable (Spitzer 1969) owing to the formation of BH binaries and the ejection of single BHs as well as the binaries in strong encounters (Kulkarni, Hut, & McMillan 1993; Sigurdsson & Hernquist 1993). However, numerical studies of star cluster evolution have shown that expansion of the BH subsystem can occur as a result of these ejections, increasing the timescale for BH evaporation and suggesting that a sizeable population of BHs can reside in present day GCs (e.g. Breen & Heggie 2013; Morscher et al. 2015). Portegies Zwart & McMillan (2000) postulated that the BH binaries that form in the centralised BH subsystem of a star cluster are ripe for merging and thus candidates for detection as GWs. The occurrence of

merges on short gravitational radiation timescales within the dense stellar environment of a cluster has been confirmed via *N*-body simulation by Aarseth (2012). It has also been shown that these BH binaries can in turn influence the overall evolution of the host cluster (Hurley & Shara 2012; Morscher et al. 2015).

Here, we introduce an *N*-body model of $N = 2 \times 10^5$ which reaches a high central density (about 10^6 stars pc^{-3}) and the end of the core-collapse phase at about 12 Gyr. This complements recent higher *N* models such as that of Wang et al. (2016) which did not reach core-collapse and previous lower density models of $N \simeq 2 \times 10^5$ (Sippel & Hurley 2013). It can also be compared to Monte Carlo models used to investigate the formation and behaviour of BH–BH binaries in star clusters (Morscher et al. 2015; Rodriguez et al. 2016b). We describe the setup of the model and general evolution characteristics in Section 2 then look specifically at the BH population within the model cluster in Section 3. In Section 4, we highlight a dynamically influenced BH–BH merger which occurred within the cluster, describing the formation pathway and outcome, then look at the effect of BH binary merges and ejection events on the behaviour of the cluster core. Finally, we compare the period distribution of dynamically formed BH–BH binaries in high- and low-density cluster models (Section 5) and discuss the results.

2 THE HIGH DENSITY *N*-BODY STAR CLUSTER

We focus here on a simulation that started with 1 95 000 single stars and 5 000 primordial binaries and was evolved to an age of 16 Gyr using the direct *N*-body code NBODY6 (Aarseth 2003; Nitadori & Aarseth 2012). The code includes algorithms to follow single and binary star evolution, as described by Hurley et al. (2001), in step with the calculation of the gravitational forces which are integrated with a fourth-order Hermite scheme. Particular attention is paid to the treatment of close encounters, with regularisation schemes and stability algorithms employed to deal efficiently with small-*N* subsystems (see Aarseth 2003 for details), whilst collisions, merges, dynamical perturbations of binary orbits, and exchange interactions, for example, are allowed.

The stellar masses are chosen from a Kroupa (2001) initial mass function (IMF) between the limits of 0.1 and 50 $M_\odot$. For the binary stars, we combine the chosen masses to give the binary mass and then redistribute the component masses according to a mass-ratio drawn at random from a uniform distribution. Orbital parameters, period, and eccentricity, are chosen according to the method described by Geller, Hurley, & Mathieu (2013) to match the observed characteristics of the binary population in the young open cluster M35. Specifically, this means that orbital periods follow the (Duquennoy & Mayor 1991) log-normal period distribution and eccentricities follow a Gaussian distribution centred on $e = 0.38$ with $\sigma = 0.23$. The metallicity chosen for the stars is $Z = 0.0002$ (or [Fe/H] $\simeq -2$). This is the metallicity of the GC NGC 6397 which is part of the metal-poor sample of Milky Way GCs (approximately 10% of the sample have lower metallicities: Bica et al. 2006). At this metallicity, stars with initial masses 18.4 $M_\odot$ or greater evolve to become BHs whilst stars of $6.1 \leq M/M_\odot < 18.4$ become neutron stars (NSs). The main-sequence turn-off mass at an age of 12 Gyr is 0.83 $M_\odot$ and stars with $0.84 < M/M_\odot < 6.1$ have evolved to become white dwarfs (WDs) by this age. All stars are assumed to be on the zero-age main sequence when the simulation begins. Stellar evolution is supplied by the Single Star Evolution (SSE) algorithm described by Hurley, Pols, & Tout (2000). We use the SSE prescription for mass loss in stellar winds except that, following the discussion by Belczynski et al. (2010), the luminous blue variable mass-loss rate for massive stars has not been applied because it overly restricts BH masses for low- to intermediate-metallicity populations. Another difference is that NS and BH remnant masses are set following the updated procedure of Belczynski et al. (2002).

It is generally assumed that NSs and possibly BHs receive a velocity kick at birth owing to asymmetries in the preceding core-collapse supernovae. The magnitude of these kicks and how they are affected by complications such as the fall-back of material during BH formation are uncertain. Some guidance can be gleaned from the observed space velocities of pulsars which are typically of the order of hundreds of km s^{-1} which, when compared to the typical escape velocity of a star cluster, of order 10 km s^{-1} or less, leads to a problem of retaining supernova remnants (Pfahl, Rappaport, & Podsiadlowski 2002). Whilst there are models that suggest a mass-dependent kick distribution for BHs (Belczynski et al. 2002), this is tempered by the results of Repetto, Davies, & Sigurdsson (2012) who find that BHs and NSs require similar kicks in order to explain the observed distribution of low-mass X-ray binaries in the Milky Way. For simplicity, we assign NSs and BHs a velocity kick at birth chosen at random from a uniform distribution between 0 and 100 km s^{-1}. The choice of natal kick distribution will have implications for the nature of the BH–BH population and this will be discussed in Section 5.

We assign the initial positions and velocities of the cluster members according to a Plummer density profile (Plummer 1911; Aarseth, Hénon, & Wielen 1974) and put the stars and binary systems initially in virial equilibrium. The half-mass radius of this starting model is 2.3 pc and the outermost star is 18.1 pc from the cluster centre.

The host galaxy is modelled as a three-component Milky Way consisting of a point-mass bulge of 1.5×10^{10} $M_\odot$ (Xue et al. 2008), a Miyamoto & Nagai (1975) disc of 5×10^{10} $M_\odot$ (Xue et al. 2008), and scale-lengths $a = 4$ kpc, $b = 0.5$ kpc, and a logarithmic dark matter halo set such that the combined mass of the bulge, disc, and halo gives a circular velocity of 220 km s^{-1} at a distance of 8.5 kpc from the Galactic centre. The sum of the contributions from the force derivatives of the three components is included directly in the force calculations, as described in Aarseth (2003). Within this host galaxy, the cluster is placed at an apogalacticon of $(x, y, z) = (7, 0, 0)$ kpc with a velocity

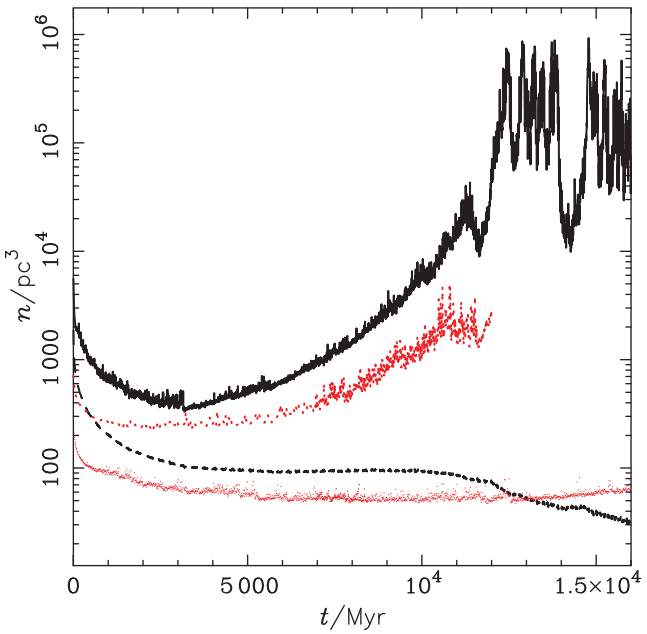

Figure 1. The stellar number density in the cluster core as a function of age for the new model presented in this work (black sold line), the Hurley & Shara (2012) model (red dotted line), and the Sippel & Hurley (2013) model (red points). Also shown for reference is the number density within the half-mass radius for the new model (dashed line).

vector $(0, 115, 45)$ km s^{-1}. So the cluster orbits between a radial distance of 2.7 to 7.0 kpc within the disc and extends to about 0.9 kpc above and below the plane of the disc. The initial mass of the cluster is 1.26×10^5 M$_\odot$. This gives a tidal radius of approximately 50 pc at apogalacticon. Accordingly, we set an escape radius of 100 pc beyond which we consider stars (or binaries) to no longer be cluster members.

After 12 Gyr of evolution the cluster mass, that of bound members, has reduced to 3.0×10^4 M$_\odot$ and at 16 Gyr it is 1.2×10^4 M$_\odot$. We note that the orbit of the model cluster is similar to that of the Milky Way GC NGC 6397 (Kalirai et al. 2007) which we used as a guide. However, the current mass of that cluster is estimated to be anywhere from 6×10^4 M$_\odot$ (Drukier 1995; Giersz & Heggie 2009) to 2.5×10^5 M$_\odot$ (Pryor & Meylan 1993), at least a factor of 2 greater than this model at a similar age.

Figure 1 describes how the stellar number density of the model evolves with cluster age. Shown are the number density within the cluster core (upper solid line) and within the half-mass radius (dashed line). Both are the number of stars divided by the relevant volume. Also shown for comparison are the core number density behaviour in the $N = 200\,000$ model of Hurley & Shara (2012) and in the $N = 250\,000$ model of Sippel & Hurley (2013). The Hurley & Shara (2012) model was evolved on a circular orbit at a distance of 3.9 kpc from the centre of the galaxy. It experienced core-collapse at an age of 10.5 Gyr and had 1.7×10^4 M$_\odot$ remaining when the simulation ended at 12 Gyr. That simulation was notable for the ejection of a BH–BH binary at about 11.5 Gyr. This caused a sharp increase in the size of the core and a corresponding drop in core number density, which is evident in Figure 1, erasing the signature of core-collapse. The Sippel & Hurley (2013) model was evolved on a circular orbit at a distance of 8.5 kpc from the centre of the galaxy. It had 6.7×10^4 M$_\odot$ of bound mass in stars and binaries remaining at an age of 12 Gyr. This model did not experience core-collapse in the 16 Gyr timeframe owing to a longer half-mass relaxation timescale compared to the other models.

It is noticeable from Figure 1 that our new model reaches a much higher central density than the previous models, at least an order of magnitude greater in fact, with the central density of the Sippel & Hurley (2013) model comparable to the half-mass radius density of the new model which in turn can be as much as four orders of magnitude less than the central density. The peak central density of the new model is about 10^6 stars pc^{-3} which is approaching that expected for the dense GCs of the Milky Way, as listed by Pooley et al. (2003). Note that luminosity densities can be converted to indicative number densities by assuming an average stellar mass of 0.5M$_\odot$ and a mass-to-light ratio of $M/L = 2\,\mathrm{M}_\odot/\mathrm{L}_\odot$ (Sippel et al. 2012).

We see a decrease in the central density over the first few Gyr of evolution as the cluster expands in response to stellar evolution induced mass loss. This is followed by a period of sustained density increase associated with the main core-collapse phase of the cluster evolution, which is interrupted briefly by a dip in density at about 11.5 Gyr (discussed below). The core-collapse phase ends at 12.2 Gyr with a central density of approximately 10^6 stars pc^{-3} and is followed by a series of core oscillations as well as a more significant drop in density at around 14 Gyr (also to be discussed below).

The corresponding core radius evolution is shown in Figure 2. We calculate the N-body core radius using the density-weighted procedure of Casertano & Hut (1985). As described by Sippel et al. (2012) fluctuations are to be expected, owing to the actions of a few massive BHs or energetic binaries in the central regions. We see from Figure 2 that, for the majority of the evolution, the core radius sits between the inner Lagrangian 1 and 10% radii, that is the radius that contains the inner 1 and 10% of the cluster mass, respectively. At late times (about 10 Gyr or later), the core radius and the 1% Lagrangian radius effectively track each other, although with some extended fluctuation in the core radius. The half-mass radius expands from its initial 2.3 pc over the first 2 Gyr of evolution and then remains fairly steady within the $4 - 5$ pc range for the remainder of the evolution. We note that the half-mass relaxation timescale (Spitzer 1987) of the initial model was 350 Myr, increasing to a maximum of about 1 500 Myr at 3.2 Gyr and decreasing to 600 Myr at 12 Gyr.

3 THE BLACK HOLE POPULATION

Approximately 380 BHs and 1 530 NSs form in the model. As mentioned above, these come primarily from stars with

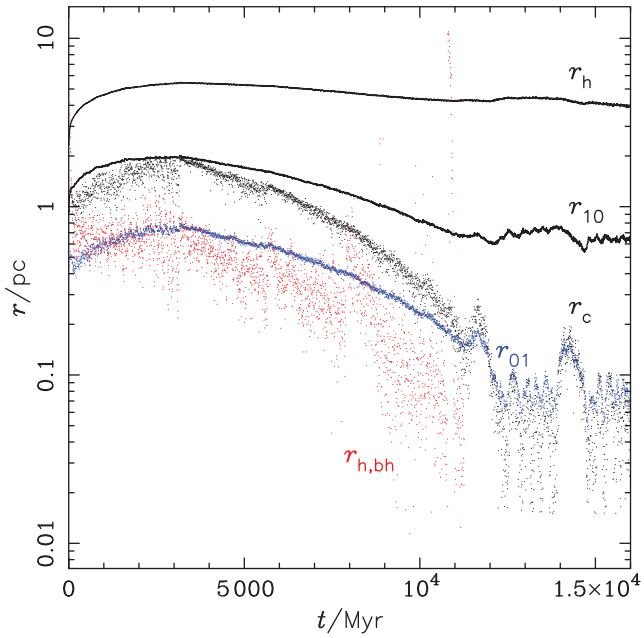

Figure 2. Evolution of various cluster radii with age: half-mass radius ($r_{\rm h}$, upper black line), inner Lagrangian 10% radius (r_{10}, lower black line), core radius ($r_{\rm c}$, black points), inner Lagrangian 1% radius (r_{01}, blue points), and the half-mass radius of the black holes ($r_{\rm h,bh}$, red points). The black hole half-mass radius is only plotted when more than two BHs are in the cluster.

initial masses in the ranges $18.4 \leq M/{\rm M}_\odot \leq 50$ and $6.1 \leq M/{\rm M}_\odot < 18.4$, respectively, with binary evolution having the ability to blur the boundaries. The first supernova occurs after about 4 Myr of evolution. At an age of 50 Myr, by which time all BHs have formed, there are 70 remaining in the cluster, a retention rate of roughly 18% after velocity kicks have been applied. NS formation continues until 120 Myr and 14% are retained at this age.

Figure 2 shows the evolution of the half-mass radius of the BH subsystem which can be compared to the half-mass radius of all stars as well as other key radii. The mass range of the BHs is typically $5 < M/{\rm M}_\odot < 30$ so they quickly become the dominant population by mass. Notably the BH half-mass radius is generally smaller than the radius containing the inner 1% of the mass of all stars, indicating that the BHs are a centrally concentrated subpopulation. In fact, both the core radius and the inner 1% Lagrangian radius exhibit a sharp decrease between 100 and 200 Myr, down to about 0.4 pc. This can be attributed to an early collapse of the BH subsystem which has its own much shorter relaxation timescale relative to the general stellar population. This behaviour has been noted by other authors in the past (Portegies Zwart & McMillan 2000; Chatterjee et al. 2016; Wang et al. 2016).

The number of BHs in the cluster steadily decreases as the cluster evolves. Of the 70 present at 50 Myr, there are 43 remaining at 1 Gyr, 20 remaining at 3 Gyr, and 10 at 7 Gyr. By the time, the cluster has reached an age of 10 Gyr only five BHs remain and at core-collapse (12.2 Gyr) there is a solitary BH in the cluster. This steady decrease of the BH population is similar to that found by Sippel & Hurley (2013) although in their lower density model, with a much longer dynamical timescale, there were 16 BHs remaining after 12 Gyr of evolution. The prime cause of the decrease is the velocity imparted to BHs in few-body encounters. This results in escape from the cluster.

The evolution of the half-mass radius of a BH subsystem was studied by Breen & Heggie (2013) using two component N-body models where all BHs have mass m_2 and all other stars have mass m_1, with $m_2 > m_1$. After the initial collapse phase of the BH subsystem they find that there is a long-lived phase of energy balance between this centralised subsystem and the remainder of the cluster. They demonstrate a relationship between the half-mass radius of the BH subsystem ($r_{\rm h,bh}$) and the overall half-mass radius ($r_{\rm h}$) in terms of the total mass in BHs (M_2) and the total mass of all other stars (M_1), where $r_{\rm h,bh}/r_{\rm h} \simeq 0.33 \left(M_2/M_1\right)^{0.28}$. For our model at 7 Gyr, an age which is well separated from the early core-collapse of the BH population and the later end of the core-collapse phase for all stars, as well as still having a sizeable BH population of 10 to ensure reasonable statistics: M_2/M_1 is 0.0011 (BHs have about 0.1% of the cluster mass). Placing this into the relationship of Breen & Heggie (2013) gives a prediction of $r_{\rm h,bh}/r_{\rm h} \simeq 0.05$ which is an excellent match to the actual value of the model. This lends credence to the validity of their relationship and means that we can assume that the BH subsystem is in the energy balance phase at this time. We note that m_2/m_1, the ratio of the average BH mass to the average stellar mass, is about 15 for our model at 7 Gyr compared to $m_2/m_1 = 10$ used by Breen & Heggie (2013) to develop their relationship. For their series of $N = 10^6$ models, Wang et al. (2016) also found consistency with the relationship of Breen & Heggie (2013), even with a higher $m_2/m_1 \simeq 40$.

4 A DYNAMICALLY INFLUENCED BLACK HOLE BINARY MERGER

As the cluster evolves BH–BH binaries form, generally through three-body encounters and exchange interactions. Of particular interest is a system that formed at 7.5 Gyr comprising BHs of mass 9.1 and 8.2 $\rm M_\odot$. These started life as single main-sequence stars of 20 and 19.5 $\rm M_\odot$ and quickly evolved to become BHs. After 4.8 Gyr of evolution, the 8.2 $\rm M_\odot$ BH formed a binary with a 1.1 $\rm M_\odot$ carbon–oxygen WD after a brief three-body interaction with the WD and a lower-mass main-sequence star. At about 7.5 Gyr with the BH–WD binary and the 9.1 $\rm M_\odot$ BH residing in the core of the cluster, a brief interaction ensues and the single BH exchanges into the binary at the expense of the WD leaving a BH–BH binary with an orbital period of about 6 800 d and an eccentricity of 0.6. Only a few Myr after formation this system is involved in a resonant exchange interaction with a third BH of mass 7.0 $\rm M_\odot$. This third BH subsequently leaves the original BH–BH intact but now with an orbital period of 410 d. The 7.0 $\rm M_\odot$ BH escapes from the cluster with a

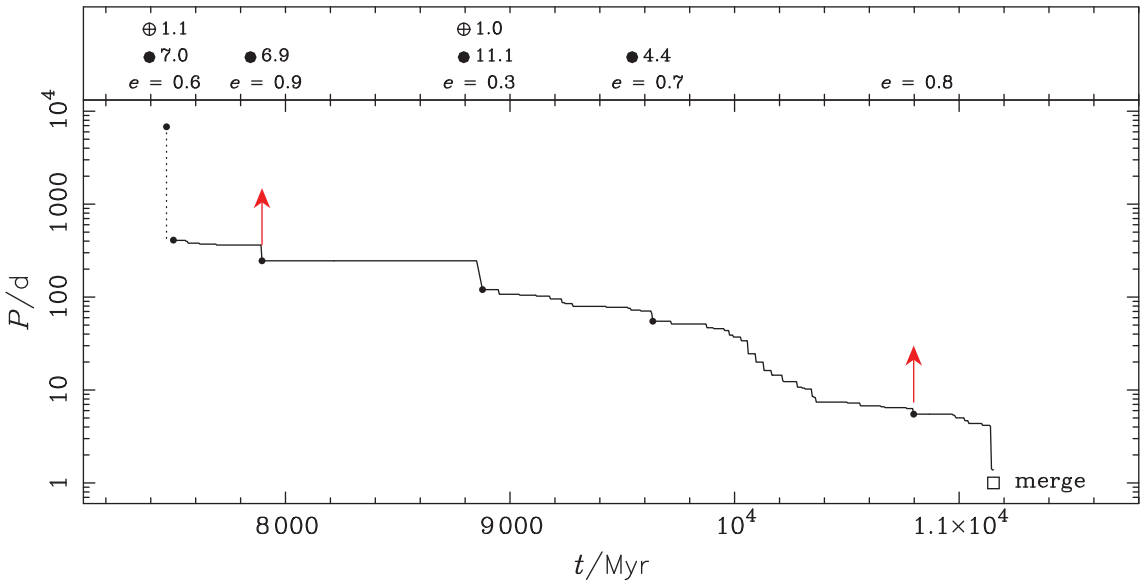

Figure 3. Period evolution of the BH–BH binary comprising 9.1 and 8.2 $M_\odot$ BHs that ends by merging. Some of the major interactions involving this system are marked along the period evolution path (corresponding to the descriptions in the text). The single stars involved in these interactions are listed above each marked point: • denotes a BH, ⊕ denotes a WD and the number is the mass of the star. The eccentricity of the BH–BH binary at the time is also given. All listed single BHs are ejected from the cluster after their interaction. The two red arrows indicate interactions in which the BH–BH binary recoils out of the cluster core.

velocity of 19.5 km s^{-1}. The BH–BH binary then remains bound until an age of 11.2 Gyr. However, in the intervening period, it suffers a succession of interactions with other stars that harden the system, reducing the orbital period and making the system more strongly bound. At formation the BH–BH binary resides in the core and successive weak encounters drive the period down to 360 d until, at around 7.9 Gyr, a stronger encounter reduces the orbital period to 245 d but also causes the binary to recoil to the outer regions of the cluster. The 6.9 $M_\odot$ single BH involved in this interaction is ejected from the cluster. By 8.9 Gyr, the BH–BH binary has sunk back into the core and a new encounter, with a 11.1 $M_\odot$ BH and a 1.0 $M_\odot$ WD, reduces the orbital period to 120 d. Successive encounters over a 2 Gyr timeframe reduce the orbital period to 6.3 d and a stronger encounter then causes a further period decrease to 5.5 d and once again pushes the binary out of the core. This explains the momentary increase in the half-mass radius of the BHs seen in Figure 2 just before 11 Gyr. Our BH–BH binary then returns to the core and further encounters reduce the orbital period to about 1 d (with an eccentricity of 0.6) at which point gravitational radiation takes over and the system quickly merges to leave a single 17.4 $M_\odot$ BH at 11.2 Gyr (under the simple assumption that no mass is lost). This is the dynamically influenced BH–BH merge—a GW source manufactured by the dense cluster environment. The evolution of the orbital period for this binary from formation to merging is shown in Figure 3 with some of the major interactions denoted. This highlights that in addition to the interactions which we have described there are many minor modifications to the orbital period as the BH–BH binary evolves.

The 17.4 $M_\odot$ BH quickly captures a companion, a 1.3 $M_\odot$ oxygen–neon WD, in an orbit that reduces from a period of 470 to 80 d over a 50 Myr interval. The eccentricity is pumped up to 0.99 and for such high eccentricity, the presence of Kozai cycles (Kozai 1962) is inevitable. Subsequently, the two stars collide at periastron and merge. We assume that all of the WD mass is added to the BH to leave a BH of mass 18.7 $M_\odot$. This more massive BH immediately captures a new companion and has a succession of partners, various WDs and a NS, before settling down with an oxygen–neon WD of mass 1.3 $M_\odot$. At an age of 11.7 Gyr, this binary escapes from the cluster with an eccentricity of 0.5 and an orbital period of 2 d. This leaves only one BH remaining in the cluster, with a mass of 5.5 $M_\odot$. At an age of 13.9 Gyr, this collides with an oxygen–neon WD whilst in a three-body system and increases its mass to 6.9 $M_\odot$. It subsequently escapes from the cluster at an age of 14.4 Gyr in a binary with another oxygen–neon WD and an orbital period of 3.1 d. The velocity of escape is 32 km s^{-1} and comes from the break-up of a three-body system in which the third star, also an oxygen–neon WD, is ejected with a velocity of 210 km s^{-1}.

As we see in Figure 2, the core radius has a local minimum at 11.3 Gyr followed by a period of expansion until 11.7 Gyr when the main core-collapse phase resumes. This timeframe of 400 Myr corresponds with the presence of the 18.7 $M_\odot$ BH in the core as a member of a binary which provides a heating effect through interactions with nearby stars.

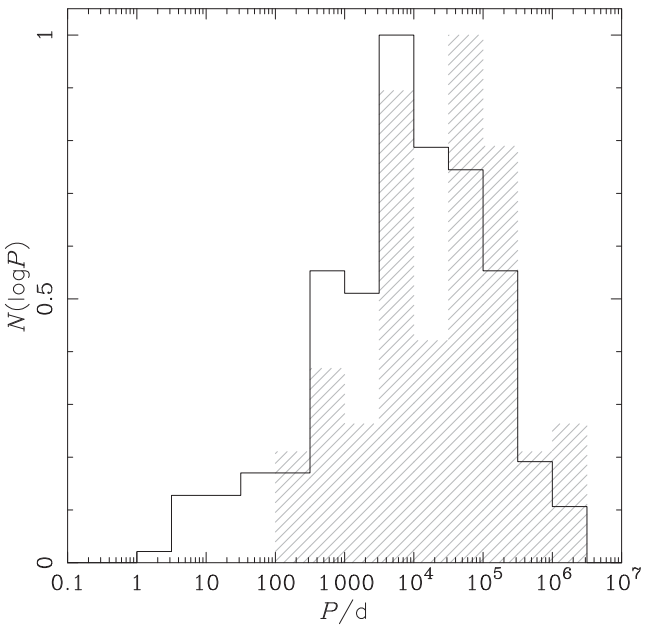

Figure 4. Period distribution of BH–BH systems at formation (hatched) and for all distinct BH–BH periods that occurred during the simulation (solid line: the *modified* distribution). Both are normalised so that the maximum number of systems in a log P bin is 1.

This ends when the BH–WD system escapes (as described above). The increase in the core radius between 13.9 and 14.4 Gyr, which temporarily halts post-core-collapse oscillations (Breen & Heggie 2014), appears to be similarly the result of heating from the BH–WD binary involving the 6.9 $M_\odot$, which escapes at 14.4 Gyr (also as described above) and leaves the cluster bereft of BHs.

5 BLACK HOLE BINARY PERIOD DISTRIBUTIONS

There are 84 distinct BH–BH binaries that form during the simulation. These are all formed dynamically with exchange interactions being the most common pathway. None come from primordial binaries even though there are some primordial binaries in which both stars are massive enough to evolve to become BHs. The mass loss during BH formation or the energy change owing to the associated velocity kicks is enough to unbind the binary in each case.

The period distribution for the 84 BH–BH binaries is shown in Figure 4. This is the period at formation for each binary. The period can subsequently undergo modification, as in the examples illustrated in the previous section. Thus, we also show the distribution of the full range of periods experienced by BH–BH binaries during the simulation. An individual binary can contribute multiple times to this *modified* distribution depending on how often its period is changed in an encounter. We see that periods of less than 100 d are only reached after formation. We find that six BH-BH binaries escape from the cluster intact over the course of the evolution. These have periods ranging from 220 to 20 000 d and are not expected to merge within a Hubble time.

For comparison, we can look at the lower density model of Sippel & Hurley (2013) which formed 50 distinct BH–BH binaries. BH–BH orbital periods less than 1 000 d were not reached in the Sippel & Hurley (2013) model and not surprisingly there were no recorded BH–BH merges in that model. That GW events are more likely to occur in high-density clusters such as our current model is to be expected because the timescale for close encounters between stars and binaries and for exchange interactions to occur is inversely proportional to the stellar number density (Hills 1992). In fact, Rodriguez et al. (2016b) have shown how the separation, or orbital period, of dynamically formed binaries is related to the cluster properties of total mass and half-mass radius, with a smaller half-mass radius leading to closer systems which are then more likely to merge (Moody & Sigurdsson 2009).

The Hurley & Shara (2012) model formed only one BH–BH binary and that subsequently escaped intact. This simulation used the Kroupa, Tout, & Gilmore (1993) IMF which, as noted by Wang et al. (2016), is less top-heavy than the Kroupa (2001) IMF, meaning a smaller proportion of massive stars and thus fewer BHs. Also, the metallicity used was $Z = 0.001$. This raises the minimum mass for BH production slightly and the lower density of the model means a lower escape velocity and thus a decreased retention rate of BHs after velocity kicks. All of these factors combined, but primarily the IMF choice, result in only a small number of BHs, four in fact, present in the Hurley & Shara (2012) model at an age of 50 Myr after comparable velocity kicks to those employed in the current model.

That all of the BH–BH binaries formed in our model are dynamical in origin compares favourably with the N-body models made by Ziosi et al. (2014) to investigate BH–BH characteristics in young star clusters. With models of $N = 5\,000$ and central densities of $10^3 - 10^4$ stars pc^{-3}, evolved over a timescale of 100 Myr, they found that 98 % or more of the BH–BH binaries formed by dynamical exchanges. They also found a period distribution primarily populated between 1 and 10^7 yr which allows for much wider systems than we find for our model shown in Figure 4.

6 SUMMARY AND DISCUSSION

So what can we infer from a single instance of a merging binary BH? Statistically we do not have a sample that allows us to compute rates, as was done by Rodriguez et al. (2016b) from a suite of Monte Carlo cluster models ranging in N from 2×10^5 to 2×10^6 stars. They found a merging rate of about 5 Gpc^{-3} yr^{-1} in the local Universe from dynamically formed BH–BH binaries in GCs and that, depending on the velocity kick imparted to BHs at birth, the rate of merging from GCs can be comparable to that from field binaries. The advantage of the Monte Carlo method

is that it allows models to be completed on a timescale of days to weeks compared to the approximately six months it took for our N-body model. For a model of similar N, initial size, and metallicity, Rodriguez et al. (2016b) found $3-4$ merges per model. In the absence of repeated instances of our N-body model and considering the stochastic nature of the dynamical formation process, our result of one merge can be taken as indicative of an expected 0–2 per model, if we did have the luxury of performing repeated models on a short enough timescale. Considering the differences in the modelling approaches, such as the treatment of the tidal field (see Giersz et al. 2013), and uncertainties involved with stellar/binary evolution (see below), this order of magnitude agreement is pleasing.

Even though the statistics of dynamically formed BH binary merges have been explored previously in Monte Carlo models, the direct confirmation and illustration of the process for an individual system in an N-body model adds to the picture. That has been the intention of this work. Going forward, there is a need to perform a wider range of N-body models to look further at how the BH–BH binary population characteristics depend on cluster properties, improve statistics, and allow a more detailed comparison with the Monte Carlo results, such as the most recent results of Rodriguez et al. (2016b). Looking closely at the sister population of BH–NS systems is also warranted. In constructing this range of models, it would be ideal if N could be varied up to 10^6 stars. Wang et al. (2016) have recently published a set of million-body simulations performed with NBODY6++GPU, a parallelised version of NBODY6 that can run across multiple GPUs. However, these models, evolved to 12 Gyr, took up to a year to run, were low density (about 10^3 stars pc^{-3}) and did not reach core-collapse. A higher density model was evolved to an age of 1 Gyr in 120 d using eight compute nodes with a combined 16 GPUs. By comparison, the $N \simeq 4\,50\,000$ model of Heggie (2014) with the standard non-parallel NBODY6 was evolved at a higher density but took over 2 yr to reach 12 Gyr. Therefore, we are not yet at the stage where we can readily perform a suite of models at large N. In the meantime, we shall focus on high-density models in the range of $N = 1\,00\,000$ to $2\,00\,000$ which will each take six or fewer months to complete.

When composing future models aimed at understanding the BH–BH binary population we need to be mindful of the results of Chatterjee et al. (2016). Their work showed that, of the various model assumptions relating to stellar and binary evolution, it is the choices for the stellar IMF and the way that post-supernova velocity kicks are applied that have the most impact, more so than the initial binary fraction and choices relating to the initial binary properties, for example. The impact of velocity kicks on BH–BH binary characteristics has also been explored recently by Belczynski et al. (2016b). Our decision to choose NS and BH velocity kicks from a uniform distribution between 0 and 100 km s^{-1} is motivated by suggestions that NS retention in rich GCs is in the range of 10–20% (Pfahl et al. 2002), as achieved by our model, and a desire for simplicity in the absence of a definitive kick model. For more massive clusters, with larger escape velocities, we would need to increase the upper limit of the uniform distribution accordingly so as to maintain retention in the 10 to 20% range. Conversely, if we were to adopt a Maxwellian distribution with a dispersion of 265 km s^{-1} (Hobbs et al. 2005) in the current model the retention fraction of NSs would be close to zero. Similarly, for BHs if they were assumed to follow suit. Given that NSs and BHs will be the heaviest cluster members and segregate to the centre of the cluster their number will affect cluster properties such as the size of the core (Breen & Heggie 2013; Chatterjee et al. 2016) as well as the characteristics of the BH–BH and BH–NS populations. As such the manner in which post-supernova velocity kicks are applied deserves serious consideration in future models.

We should also be prepared to relax the upper limit to the stellar IMF and allow initial masses up to 100 $M_\odot$ in future models. For the Kroupa (2001) IMF that we have adopted, less than 0.05% of stars lie in the 50 to 100 $M_\odot$ range, meaning that our decision to cap the IMF at 50 $M_\odot$ has deprived the model of about 50 higher mass stars that would have been present if we had extended the IMF to 100 $M_\odot$. This high-end truncation will affect the mass spectrum of the BHs that are produced, assuming they are retained in the cluster, and in turn will have an impact on results such as the timescale of BH ejection and the cluster evolution (e.g. Morscher et al. 2015). Increasing the upper limit to the IMF and widening the range of BH masses in the model will also increase the applicability to the detection results. The LIGO BH–BH binary GW detection GW150914 (Abbott et al. 2016a) has component masses of around 30 $M_\odot$ and a chirp mass of 28 $M_\odot$. Our BH–BH merger has a lower chirp mass of 7.5 $M_\odot$ coming from BHs of the order of 10 $M_\odot$. It is within the range of the masses derived for the subsequent GW detection GW151226 (Abbott et al. 2016b).

Within our NBODY6 treatment, the gravitational radiation timescale for close binary systems is given by the classical Peters (1964) expression and implemented in terms of changes to the orbital angular momentum and the eccentricity (Hurley, Tout, & Pols 2002). Whilst this is accurate enough for our current purpose, a more accurate treatment involving post-Newtonian terms is available in the sister code NBODY7 (Aarseth 2012). Newtonian dynamics can initiate substantial shrinkage of the orbital separation but a favourable timescale for merging is enhanced by high eccentricity which implies that Kozai cycles (Kozai 1962) will be present. In this case, the post-Newtonian treatment would ensure greater accuracy for the modelling of the final stages (see Aarseth 2012).

Our model reaches the end of the main core-collapse phase at an age of roughly 12 Gyr and has only one BH remaining at this late dynamical time. Shortly afterwards, it has completely lost the BH population. This is consistent with predictions from theory and scattering experiments that model the behaviour of the BH subsystem that old GCs would retain

at most a few BHs (e.g. Kulkarni et al. 1993; Sigurdsson & Hernquist 1993). It is also consistent with the *N*-body model of Heggie (2014) which had lost its BH population at about the time that the main core-collapse phase ended. In contrast, the less evolved model of Sippel & Hurley (2013) had 16 BHs remaining at 12 Gyr and the million-body models of Wang et al. (2016), also less evolved but with a more generous BH retention rate owing to the chosen application of velocity kicks, contained of the order of a few hundred to a thousand BHs. The set of Monte Carlo models published by Morscher et al. (2015) also showed that thousands of BHs could be retained in GCs, with some dependence on cluster properties and again with a generous retention rate. These results highlight the difference between dynamically old and dynamically young clusters in terms of expected BH population numbers and the need to further understand how these numbers and properties depend on the nature of cluster evolution.

Whilst our model shows much dynamical activity involving BHs, including the dynamically formed GW source that we have highlighted, what is surprising is that we see little evidence for heightened dynamical production of some other exotic binary populations. For example, the model contains zero cataclysmic variables and low-mass X-ray binaries at 12 Gyr. Given the higher density of the model compared to earlier simulations and in light of the long-held suggestion that a dense stellar environment should produce an increase in compact binaries (e.g. Fabian, Pringle, & Rees 1975; Davies 1997; Pooley et al. 2003), these non-detections are surprising. This definitely requires further investigation. Most likely the particulars of the primordial binary population, for example, the choice of a uniform mass-ratio distribution, and how this interacts with the stellar environment are important for the production of these types of systems, but not for BH–BH binaries (Chatterjee et al. 2016).

ACKNOWLEDGEMENTS

JRH would like to thank Churchill College for a Visiting By-Fellowship and the Institute of Astronomy visitor programme for facilitating this work. CAT thanks Churchill College for his fellowship. This work was performed on the gSTAR national facility at Swinburne University of Technology. gSTAR is funded by Swinburne and the Australian Governments Education Investment Fund.

REFERENCES

Aarseth, S. J. 2003, Gravitational N-body Simulations: Tools and Algorithms, Cambridge Monographs on Mathematical Physics (Cambridge: Cambridge University Press)
Aarseth, S. J. 2012, MNRAS, 422, 841
Aarseth, S., Hénon, M., & Wielen, R. 1974, A&A, 37, 183
Abbott, B. P., et al. 2016a, PhRvL, 116, 061102
Abbott, B. P., et al. 2016b, PhRvL, 116, 241103
Antonini, F., Chatterjee, S., Rodriguez, C. L., Morscher, M., Pattabiraman, B., Kalogera, V., & Rasio, F. A. 2016, ApJ, 816, 65
Belczynski, K., Bulik, T., Fryer, C. L., Ruiter, A., Valsecchi, F., Vink, J. S., & Hurley, J. R. 2010, ApJ, 714, 1217
Belczynski, K., Holz, D. E., Bulik, T., & O'Shaughnessy, R. 2016a, Nature, 534, 512
Belczynski, K., Kalogera, V., & Bulik, T. 2002, ApJ, 572, 407
Belczynski, K., Repetto, S., Holz, D. E., O'Shaughnessy, R., Bulik, T., Berti, E., Fryer, C., & Dominik, M. 2016b, ApJ, 819, 108
Bica, E., Bonatto, C., Barbuy, B., & Ortolani, S. 2006, A&A, 450, 105
Breen, P. G., & Heggie, D. C. 2013, MNRAS, 432, 2779
Casertano, S., & Hut, P. 1985, ApJ, 298, 80
Chatterjee, S., Rodriguez, C. L., & Rasio, F. A. 2016, arXiv:1603.00884
Davies, M. B. 1997, MNRAS, 288, 117
Dominik, M., et al. 2015, ApJ, 806, 263
Downing, J. M. B., Benacquista, M. J., Giersz, M., & Spurzem, R. 2011, MNRAS, 416, 133
Drukier, G. A. 1995, ApJS, 100, 347
Dvorkin, I., Vangioni, E., Silk, J., Uzan, J.-P., & Olive, K. A. 2016, MNRAS, 461, 3877
Duquennoy, A., & Mayor, M. 1991, A&A, 248, 485
Eldridge, J. J., & Stanway, E. R. 2016, arXiv:1602.03790
Fabian, A., Pringle, J. E., & Rees, M. J. 1975, MNRAS, 172, 15
Geller, A. M., Hurley, J. R., & Mathieu, R. D. 2013, AJ, 145, 8
Giersz, M., & Heggie, D. C. 2009, MNRAS, 395, 1173
Giersz, M., Heggie, D. C., Hurley, J. R., & Hypki, A. 2013, MNRAS, 431, 2184
Heggie, D. C. 2014, MNRAS, 445, 3435
Hills, J. G. 1992, AJ, 103, 1955
Hobbs, G., Lorimer, D. R., Lyne, A. G., & Kramer, M. 2005, MNRAS, 360, 974
Hurley, J. R., Pols, O. R., & Tout, C. A. 2000, MNRAS, 315, 543
Hurley, J. R., Tout, C. A., Aarseth, S. J., & Pols, O. R. 2001, MNRAS, 323, 630
Hurley, J. R., & Shara, M. M. 2012, MNRAS, 425, 2872
Hurley, J. R., Tout, C. A., & Pols, O. R. 2002, MNRAS, 329, 897
Kalirai, J. S., et al. 2007, ApJ, 657, L93
Kozai, Y. 1962, AJ, 67, 591
Kroupa, P. 2001, MNRAS, 322, 231
Kroupa, P., Tout, C. A., & Gilmore, G. 1993, MNRAS, 262, 545
Kulkarni, S. R., Hut, P., & McMillan, S. 1993, Nature, 364, 421
Mapelli, M. 2016, MNRAS, 459, 3432
Miyamoto, M., & Nagai, R. 1975, PASJ, 27, 533
Moody, K., & Sigurdsson, S. 2009, ApJ, 690, 1370
Morscher, M., Pattabiraman, B., Rodriguez, C. L., Rasio, F. A., & Umbreit, S. 2015, ApJ, 800, 9
Nitadori, K., & Aarseth, S. J. 2012, MNRAS, 424, 545
Peters, P. C. 1964, PhRv, 136, B1224
Pfahl, E., Rappaport, S., & Podsiadlowski, P. 2002, ApJ, 573, 283
Plummer, H. C. 1911, MNRAS, 71, 460
Pooley, D., et al. 2003, ApJ, 591, L131
Portegies Zwart, S. F., & McMillan, S. L. W. 2000, ApJ, 528, L17
Pryor, C., & Meylan, G. 1993, in ASP Conf. Ser., 50, Structure and Dynamics of Globular Clusters, ed. S. G. Djorgovski, & G. Meylan (San Francisco: ASP), 357
Repetto, S., Davies, M. B., & Sigurdsson, S. 2012, MNRAS, 425, 2799
Rodriguez, C. L., Chatterjee, S., & Rasio, F. A. 2016a, Physical Review D, 93, 084029

Rodriguez, C. L., Haster, C.-J., Chatterjee, S., Kalogera, V., & Rasio, F. A. 2016b, ApJ, 824, L8
Sigurdsson, S., & Hernquist, L. 1993, Nature, 364, 423
Sippel, A. C., & Hurley, J. R. 2013, MNRAS, 430, L30
Sippel, A. C., Hurley, J. R., Madrid, J. P., & Harris, W. E. 2012, MNRAS, 427, 167
Spitzer, L. 1969, ApJ, 158, L139
Spitzer, L. Jr. 1987, Dynamical Evolution of Globular Clusters (Princeton: Princeton University Press)
Wang, L., et al. 2016, MNRAS, 458, 1450
Xue, X. X., et al. 2008, ApJ, 684, 1143
Ziosi, B. M., Mapelli, M., Branchesi, M., & Tormen, G. 2014, MNRAS, 441, 3703